Order parameter in incommensurate Rb_2ZnCl_4 studied by Mn^{2+} electron paramagnetic resonance

J. J. L. Horikx, A. F. M. Arts, and H. W. de Wijn
Fysisch Laboratorium, Rijksuniversiteit Utrecht, P.O. Box 80.000, 3508 TA Utrecht, The Netherlands
(Received 21 October 1987)

The incommensurate modulation in Rb_2ZnCl_4, which involves rotations of slightly distorted $ZnCl_4$ tetrahedra, is examined below the normal-to-incommensurate transition at $T_1 = 30.42 \pm 0.04$ °C via the associated distribution of resonance fields in the EPR of Mn^{2+} ions dilutely substituted for Zn^{2+}. The analysis is based on the spin Hamiltonian appropriate to Mn^{2+} in a rhombic crystalline field. Excellent reproduction of the experimental spectra is obtained by summing over the calculated spectra of the individual Mn^{2+} on the assumptions of a sinusoidal modulation wave, a fine-structure tensor rotating with the tetrahedra, and a linewidth independent of the phase of the modulation. Further, allowance is made for small additional deformations of the tetrahedra induced by the modulation. The order parameter Q, i.e., the amplitude of the modulation wave, increases to 8° of arc at 8 K below T_1. Its temperature dependence is in conformity with classical Landau theory provided the free energy is expanded up to the sixth power in Q. Further, data on the linewidth are presented around T_1. Above T_1, $D = 480 \pm 5$ G and $E = -27 \pm 5$ G.

I. INTRODUCTION

This paper is concerned with the order parameter associated with the modulation wave in Rb_2ZnCl_4 as determined with electron paramagnetic resonance (EPR) in the regime just below the normal-to-incommensurate transition, and with an interpretation of the results in terms of the classical Landau theory. Rb_2ZnCl_4 belongs to the family of compounds with the β-K_2SO_4 structure, many members of which exhibit a transition to an incommensurate phase.[1,2] In the high-temperature normal phase, Rb_2ZnCl_4 is orthorhombic with space group D_{2h}^{16} (*Pmcn*; choice of axes such that $b > c > a$).[3,4] The unit cell contains 4 formula units, and the Zn ions reside within slightly deformed $ZnCl_4$ tetrahedra located on (b,c) mirror planes. Below $T_1 = 303.6$ K an incommensurate displacive modulation with wave vector $\mathbf{q}_i = (\frac{1}{3} - \delta)\mathbf{c}^*$ develops, with $\delta = 0.029$ just below the transition.[5,6] The modulation involves reorientations of the tetrahedra as well as displacements of the Rb ions.[4] Towards lower temperatures δ decreases, until at the lock-in transition at $T_2 = 192$ K it drops to zero. The modulation is sinusoidal not too far below T_1 (plane-wave limit), whereas closer to the lock-in transition higher harmonics develop and the modulation is better described by an array of phase solitons.[7-10] The average structure in the incommensurate phase has the space group of the high-temperature normal phase.[11]

The method used to probe the incommensurate wave is to observe modifications of the fine-structure splittings of the EPR of Mn^{2+} ions randomly substituted for Zn^{2+} to dilute concentrations. The present analysis relies on the well-established spin Hamiltonian of individual Mn^{2+} ions in a crystalline field of rhombic symmetry. The shifts of the EPR transitions of these ions are calculated on the basis of a microscopic model of the incommensurate modulation with the amplitude of the rotations of the tetrahedra as order parameter. The crystalline field is primarily generated by the immediate surroundings of the resonant ion, and in the present case is caused by the deformed tetrahedra. EPR thus senses the tetrahedral rotations associated with the incommensurate wave through a reorientation of the fine-structure tensor reflecting the rhombic symmetry. A distribution of resonance fields results, the width of which reflects the order parameter. Excellent fits are obtained by summing over the various local contributions of the individual Mn^{2+} with the linewidth taken constant, provided small deformations additional to those already present in the high-temperature normal phase are taken into account.

EPR of Mn^{2+} in Rb_2ZnCl_4 has earlier been examined in some detail, chiefly by Fayet and co-workers.[12-14] The analysis adopted in Ref. 13, which is the most relevant in connection with the present study, is distinct from the approach below in that the EPR line shapes below T_1 are analyzed in terms of a phenomenological expansion of the resonance field in powers of the local displacements, while the linewidth is let to vary with the local phase of the modulation wave to arrive at satisfactory simulations of the experimental profiles. It is further noted that the temperature dependence of the order parameter has earlier been examined via the spread the associated quadrupolar shifts cause in the NMR of the Rb nuclei.[8,15] The results appeared to be reconcilable with a rise of the order parameter according to a simple power law with critical exponent $\beta \approx 0.35$.

II. EXPERIMENTAL RESULTS

The spectra were recorded with a superheterodyne EPR spectrometer operating at a fixed frequency of 23.900 GHz, and equipped with phase-sensitive detection of the 60-MHz intermediate frequency to minimize noise. The frequency of the primary klystron, phase locked to a harmonic of a quartz reference oscillator, was set to reso-

nance with the cylindrical microwave cavity, resonating in the TE_{011} mode, in which the sample was mounted. Field modulation at about 30 Hz was applied so that the derivative spectrum was observed. The latter was digitized and accumulated in a multichannel analyzer. The temperature of the sample cavity was servostabilized to within 0.04 K. The sample, having a volume of about 2 mm^3, was cut from a boule grown with the Stockbarger method. The Mn^{2+} content, determined with atomic absorption, is 0.2 at. %.

The spin Hamiltonian appropriate to Mn^{2+} ($S=\frac{5}{2}$, $I=\frac{5}{2}$) in a crystalline field of rhombic symmetry may, with reference to the principal axes, denoted by x, y, and z, be written

$$\mathcal{H}=g\mu_B\mathbf{H}\cdot\mathbf{S}+D[S_z^2-\tfrac{1}{3}S(S+1)]+E(S_x^2-S_y^2)+A\mathbf{S}\cdot\mathbf{I}\ . \tag{1}$$

Here, D and E are the fine-structure constants ($|E/D|<1$), while A is the ^{55}Mn hyperfine constant. This Hamiltonian generally gives rise to an EPR spectrum consisting of $2S$ groups of $2I+1$ hyperfine lines. When expressed in resonance fields, the latter are at a mutual distance of approximately $|A|/g\mu_B$. The hyperfine groups are in first order separated by

$$|D(3\cos^2\theta'-1)-3E(\cos^2\theta'-1)\cos2\phi'|/g\mu_B\ , \tag{2}$$

where θ' and ϕ' are the polar and azimuthal angles of the external field with reference to x, y, and z.

In the present case, Mn^{2+} is within a deformed tetrahedron of Cl^-. In the high-temperature phase, there are, for the sake of EPR, two inequivalent classes of sites, which differ in the orientations of the principal axes of their D tensors. For reasons of symmetry, each D tensor has two of its principal axes within the (b,c) mirror plane, however in such a way that the D tensors of the two classes are tilted away from the c axis by equal amounts to either side. An appropriate choice of the x, y, and z axes is displayed in Fig. 1. Rotational diagrams of the EPR at 313 K, well above T_1, are displayed in Fig. 2 after removal of the hyperfine structure. By fitting the fine-structure part of Eq. (1) to the diagrams, we derive $D/g\mu_B=+480\pm5$ G and $E/g\mu_B=-27\pm5$ G, while the tilt angle of the z axis, θ_0, is found to amount to $4.6°\pm0.5°$ of arc. From the hyperfine structure we find

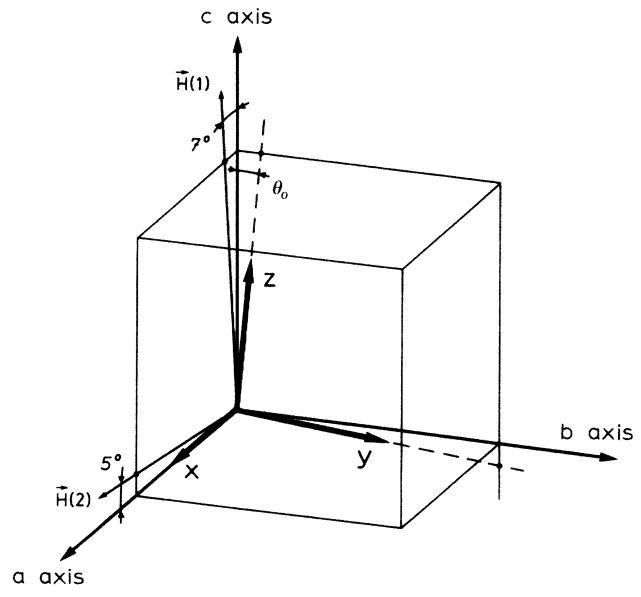

FIG. 1. Orientation of the D-tensor principal axes of Mn^{2+} in Rb_2ZnCl_4 relative to the crystal axes for one of the two classes of inequivalent sites; the orientation pertaining to the other class is the mirror image about the (a,c) plane. Also shown are two directions of the magnetic field, labeled (1) and (2).

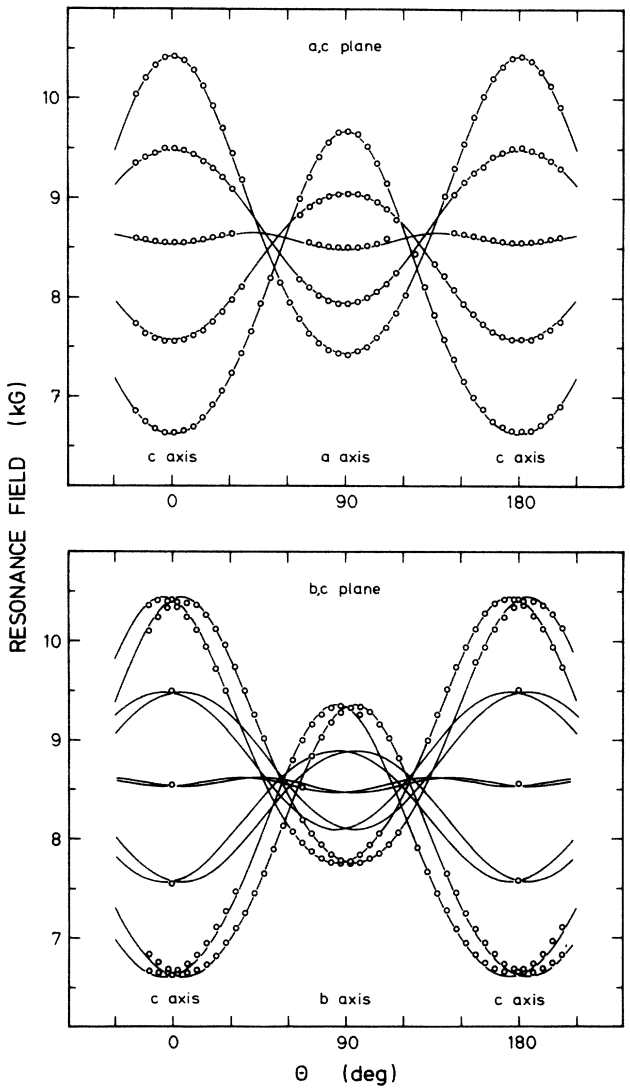

FIG. 2. Rotational diagrams of the fine structure of the EPR of Mn^{2+} in Rb_2ZnCl_4 in the high-temperature phase at 313 K for **H** oriented in the (a,c) plane (upper frame) and in the (b,c) plane (lower frame). Solid lines are fits with $D/g\mu_B=+480$ G and $E/g\mu_B=-27$ G.

$A/g\mu_B = -77.2 \pm 0.5$ G, where we have adopted the negative sign pertinent to Mn^{2+}. Given the sign of A, the second-order hyperfine structure, which invokes shifts of order $A^2/g\mu_B H$,[16] allows to assign unequivocally the quantum numbers M_S to each hyperfine sextuplet, and thus to determine the absolute sign of the fine-structure splittings. As a case in point, the outermost hyperfine separations of the $M_S = +\frac{5}{2} \leftrightarrow +\frac{3}{2}$ transitions amount to $|A + 4A^2/g\mu_B H|$ and $|A|$, while those of $M_S = -\frac{3}{2} \leftrightarrow -\frac{5}{2}$ are $|A|$ and $|A - 4A^2/g\mu_B H|$. We thus deduce $D > 0$, which we have anticipated in the results for D and E derived from Fig. 2 above.

In the incommensurate phase, the directional spread of the D-tensor principal axes due to the reorientation of the tetrahedra gives rise to a distribution of resonance fields of the outer four fine-structure transitions. (The central $M_S = +\frac{1}{2} \leftrightarrow -\frac{1}{2}$ transition is affected much more weakly, its shift containing an additional factor of order $D/g\mu_B H$.) In order to simplify the analysis of the EPR spectra, it is expedient to make the distributions associated with the two inequivalent classes of Mn^{2+} sites coincide by taking **H** in the (a,c) or (a,b) planes. Of these, the (a,c) plane is the most practical because it also is a cleavage plane, facilitating alignment of the crystal. As for the further selection of **H**, it is, on the one hand, desirable that its orientation be close to one of the principal axes of the D tensor so as to avoid overlap of the adjacent hyperfine sextuplets (cf. Fig. 2). On the other hand, the orientation of **H** should be sufficiently out of the (b,c) plane, as well as away from the a axis, for the EPR displacements to become of sizable magnitude and to become in lowest-order linear with the rotation. Experimentally convenient compromises for the directions of **H**, used in the present study, are indicated in Fig. 1. As an example of the measured development of the EPR spectra with temperature, spectra containing the lowest-resonance-field transition ($M_S = -\frac{3}{2} \leftrightarrow -\frac{5}{2}$, $m_I = -\frac{5}{2}$) are collected in Fig. 3 from 31.5 down to 23.4 °C for **H** in the (a,c) plane at 5° off the a axis [$\theta = 85°$, $\phi = 0°$; orientation (2)]. In the analysis, emphasis is laid on the outermost lines of the various hyperfine groups to minimize overlap of neighboring lines.

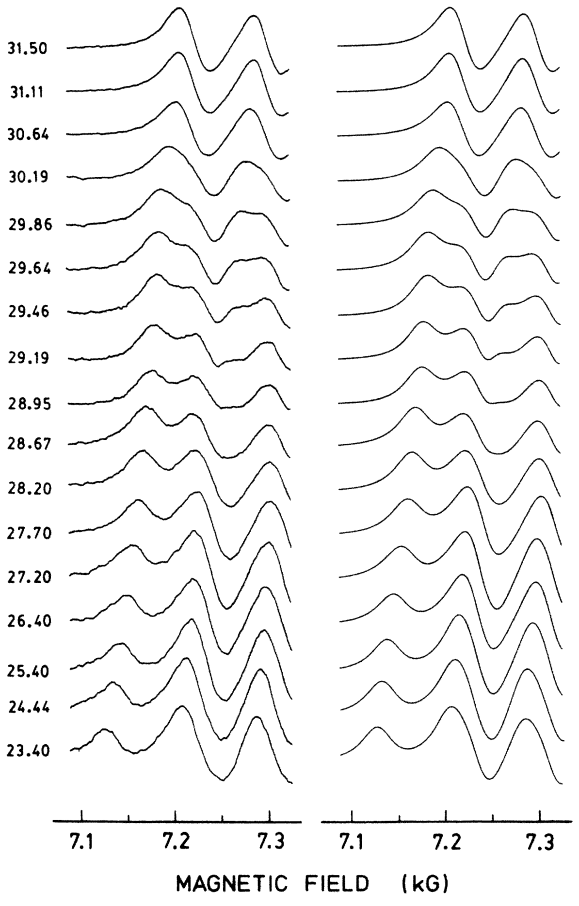

FIG. 3. Experimental spectra (left) and simulated spectra (right) near the lowest-resonance-field $M_S = -\frac{3}{2} \leftrightarrow -\frac{5}{2}$, $m_I = -\frac{5}{2}$ transition for **H** directed along direction (2) as in Fig. 1. Number entries represent temperatures in degrees centigrade. Below $T_1 = 30.42$ °C, the spectra reflect the distribution of resonance fields associated with the incommensurate modulation. The experimental spectra have been accumulated with different numbers of scans.

III. ANALYSIS OF THE SPECTRA

In order to describe the incommensurate orientational distribution of the tetrahedra, or, more precisely, of the D-tensor principal axes, we introduce a vector ω, representing the rotation of the principal axes relative to the crystal axes as a function of the phase $\mathbf{q}_i \cdot \mathbf{r}$ of the modulation wave. The components of this vector, here taken with reference to the crystal axes, can be written as a Fourier series in $\mathbf{q}_i \cdot \mathbf{r}$. Some restrictions on the Fourier coefficients are imposed by symmetry. Although the modulation destroys the (b,c) mirror symmetry locally, the average structure of the incommensurate phase still has the space group of the high-temperature normal phase. The (b,c) plane, therefore, remains a mirror plane as far as the *distribution* of the orientations of the principal axes is concerned. The Fourier series for ω_b and ω_c contain only terms of odd order, whereas in the Fourier series for ω_a only terms of even order are allowed. In the plane-wave limit, i.e., retaining the lowest-order terms only, the rotation of the principal axes is then given by

$$\omega = Q(\alpha, \sin(\mathbf{q}_i \cdot \mathbf{r}),\ \gamma \sin(\mathbf{q}_i \cdot \mathbf{r} + \delta)) , \tag{3}$$

in which the amplitude of the rotation about the b axis is identified with the order parameter Q. The components ω_b and ω_c thus describe the incommensurate orientational distribution, while $Q\alpha$ allows to account for a temperature-dependent change of the tilt angle. Equation (3) refers to the tetrahedra with tilt angle θ_0. For the sites with opposite tilt angle, α and γ have to be reversed in sign. It is noted that for the isostructural compound K_2SeO_4 a rotation vector of the form expressed by Eq. (3) has been found adequate in an x-ray structural study of the incommensurate phase.[17]

Prior to simulating the effects of the incommensurate modulation on the EPR spectra, we observe that rotations of the D tensor about the c axis produce appreciably more narrow distributions of resonance frequencies than do b-axis rotations. From considerations relying on Eq. (2) and Fig. 1 it may be estimated that the difference is by a factor of order $|2E/D| \sim 0.1$. Simulations such as the ones described below, which account more precisely for the misalignment of the D tensor relative to the crystalline axes, yield a factor of 0.08 for the effects of c-axis over b-axis rotations in the case the field is along direction (1), and 0.07 in the case it is along direction (2). In effect, the sensitivity of the EPR for c-axis rotations alone is so small that the observed distributions cannot be spanned, not even for rotations over 90°. Further, the analysis indicates that the temperature dependence of the average positions of the experimental fine-structure groups is entirely accounted for by a simulation with α set to zero, inferring α to be small. We, therefore, restrict the rotations of the tetrahedra to rotations about the b axis, i.e., $\alpha=0$ and $\gamma=0$, noting that what effects of c-axis rotations are left may be absorbed in those of the b-axis rotations. The procedure is to some extent heuristic, but is lent justification in the excellent resemblance of the theoretical and experimental spectra for all directions of **H** considered with a unique set of fitted parameters.

The straightforward method to evaluate the theoretical spectra then is (i) to let the orientation of the principal axes of the D tensor be distributed according to the rotation $Q\sin(\mathbf{q}_i\cdot\mathbf{r})\,\mathbf{e}_b$, while adopting a uniform distribution of the Mn^{2+} ions over the modulation wave, (ii) to calculate the corresponding distribution of resonance fields from Eq. (1) given the spin-Hamiltonian parameters and the orientation of the field, and (iii) to convolute the result with a Lorentzian accounting for the finite linewidth. As it turns out, however, spectra calculated in this way do not reproduce the measured spectra in all details. The range of the resonance positions produced by the incommensurate modulation appears to be consistent with experiment, but the intensity distribution is at fault for **H** pointing in directions near the a axis and, to a lesser extent, directions near the c axis. In addition to *rotations* of the D tensor, we have therefore considered variations of the *magnitudes* of the parameters D and E with the incommensurate wave. That is, we have allowed for an additional distortion of the tetrahedra, which, in a local approximation, may be expanded in a power series of the departure of the tetrahedra from the high-temperature orientation. By virtue of the symmetry, terms odd in the deviation angle are absent, so that, to lowest order, D and E may be written

$$\begin{aligned} D &= D_0 + D_2 Q^2 \sin^2(\mathbf{q}_i\cdot\mathbf{r}) \,, \\ E &= E_0 + E_2 Q^2 \sin^2(\mathbf{q}_i\cdot\mathbf{r}) \,. \end{aligned} \tag{4}$$

Here, D_0 and E_0 equal the values of D and E above T_1.

The calculation of the theoretical spectra has been implemented on computer in the following way. First, given Q and the orientation of **H** with reference to the crystalline axes, the angles θ and ϕ are computed for 16 values of $\mathbf{q}_i\cdot\mathbf{r}$ equally spaced over the interval $0-2\pi$. Next, for each of these geometries the fine-structure part of the spin Hamiltonian, Eq. (1), is diagonalized exactly, and the energy separations associated with the five fine-structure transitions are calculated. Since in the actual experiments one measures resonance fields at a fixed frequency rather than energy separations, this is done for five suitably chosen values of H. The resonance fields, i.e., the fields for which the energy separations equal the microwave quantum, are then derived by Lagrange interpolation. Analytical expressions for the resonance fields as a function of $\mathbf{q}_i\cdot\mathbf{r}$ are subsequently constructed in the form of Fourier series based on the 16 values of $\mathbf{q}_i\cdot\mathbf{r}$ selected. The simulated shape of the resonance line as broadened by the incommensurate modulation with amplitude Q is finally found by making up a histogram of the resonance fields corresponding with at least 50 equidistant $\mathbf{q}_i\cdot\mathbf{r}$ covering a full period of the modulation, introducing the hyperfine structure by adding six of the resultant line shapes shifted to mutual distance A, and convoluting the hyperfine sextuplets with the derivative of a Lorentzian of specified width. In the last step, the Lorentzian is in part replaced by its dispersive counterpart to the extent necessary.

The theoretical spectra have been least-squares adjusted to the measured spectra. In each case, the fitting parameters are Q, D_2, E_2, and the linewidth, besides the trivial ones, such as scaling factors and a parameter expressing that the spectra appear to contain a small dispersive component in addition to the absorptive one. Examples of the fitted line shapes in the case of orientation (2) in Fig. 1 are presented and compared with experiment in Fig. 3. For orientation (1) fits of similar quality (not shown here) have been achieved. The most prominent result is that for both orientations of **H** considered the above model of rotating tetrahedra is able to provide a perfect description of the experimental spectra. The output values for Q, the quantity of primary interest in this paper, are displayed in Fig. 4. It is noteworthy that the development of Q with the temperature as derived from the spectra with **H** near the c axis [orientation (1)] coincides with the results for Q from near-a-axis spectra [orientation (2)]. As concerns the magnitude of the effects, at 3 °C below the transition, for instance, Q is found to amount to 6°, corresponding with displacements of the Cl ions of 0.1–0.2 Å. As noted above, rotations of the D tensor about the c axis would contribute to Q, yet 10–15 times less effectively than comparable b-axis rotations. A neutron structural study of the present system in the lock-in phase,[4] as well as an x-ray analysis of the modulated phase of the isostructural compound Rb_2ZnBr_4,[2] indicate c-axis rotations to be about twice as large as b-axis rotations. Accordingly, the true rotation angle about the b axis possibly deviates from Q by 15% at most. The quantities D_2 and E_2, which are determined most significantly from the spectra with orientations (1) and (2), respectively, are given in Fig. 5 as a function of Q. These results suggest constancy of the parameters D_2 and E_2 up to $Q\approx 6°$, beyond which point both D_2 and E_2 increase. These departures of D_2 and E_2, which supposedly result from the omission of higher-order terms in Eqs. (4), do however not markedly deteriorate the fits at

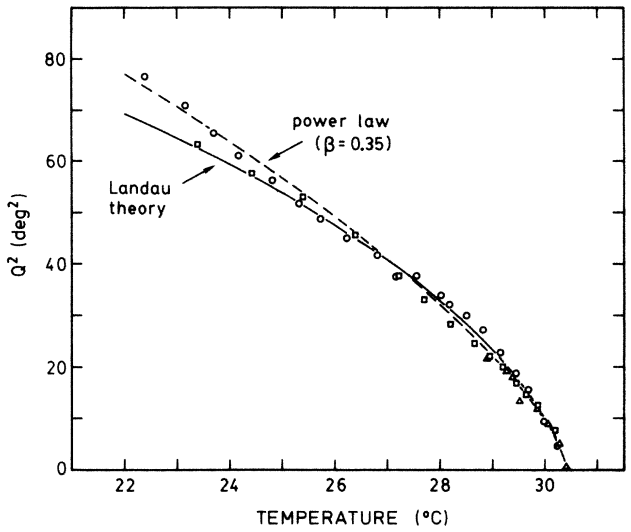

FIG. 4. Squared amplitude of the b-axis rotation of the tetrahedra, Q^2, vs the temperature, as derived from the resonance profiles at the low-field side of hyperfine sextuplets; (○) $M_S=-\frac{1}{2}\leftrightarrow-\frac{3}{2}$ and **H** pointing along direction (1) as in Fig. 1; (△) $M_S=-\frac{3}{2}\leftrightarrow-\frac{5}{2}$ and **H** along direction (1); (□) $M_S=-\frac{3}{2}\leftrightarrow-\frac{5}{2}$ and **H** along direction (2). Solid and dotted lines are adjustments of the Landau theory, Eq. (6), and a power law to the data above 24.5 °C, respectively.

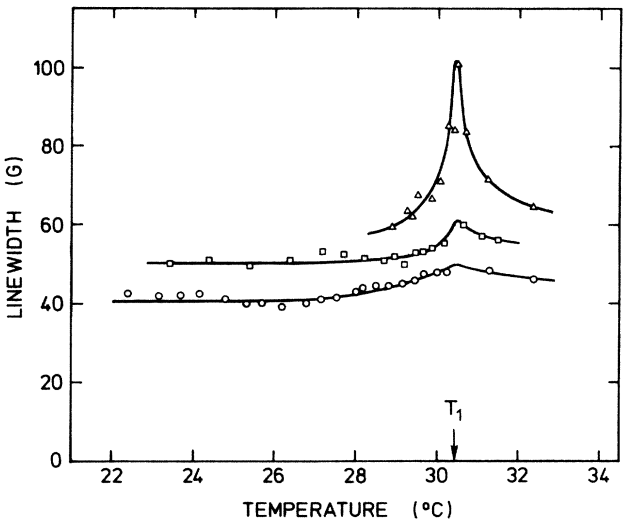

FIG. 6. Temperature dependence of the full width at half maximum of the Lorentzians convoluted with the calculated resonance-field distributions. The points are the results from the fits yielding Q^2 in Fig. 4. Above T_1, Q has been set to zero. Symbols are as in Fig. 4. Lines are guides to the eye.

the higher Q (cf. Fig. 3). Some results for the linewidth are given in Fig. 6.

We have further analyzed some spectra with **H** pointing along the a and b axes. These spectra are of interest in that they provide additional evidence for the modification of the quantities D and E with the orientation, as expressed by Eqs. (4). Unlike the cases treated above, in these geometries the field does not break the (b,c) mirror symmetry. Accordingly, the EPR fine-structure shifts associated with the incommensurate rotation are, as are the shifts due to D_2 and E_2, to lowest-order quadratic in the rotations.[18] In the case of **H** parallel to the a axis, calculations based on the fitted parameters indicate that the spread of the resonance fields of the highest-field $M_S=+\frac{5}{2}\leftrightarrow+\frac{3}{2}$, $m_I=+\frac{5}{2}$ transition due to reorientation of the z principal axis alone would have grown to 45 G at $Q=6°$, but further that this spread is nearly nullified by the effects of D_2 and E_2. This, indeed, is in accord with what is observed. This finding to some extent also corroborates the smallness of γ relative to $|D/2E|\sim 10$, as assumed in the analysis. Even firmer support for D_2 and E_2 is lent by the spectra with **H** pointing along the b axis. These spectra are, of course, insensitive to any rotation about the b axis, and, as calculations confirm, are virtually independent of c-axis rotations for realistic rotation angles. Yet a significant line broadening, of order 20 G in width, is observed in going from T_1 down to 27 °C, which again is consistent with the calculated effects from D_2 and E_2. The absence of a uniform shift in these spectra further indicates that $\alpha \ll 1$.

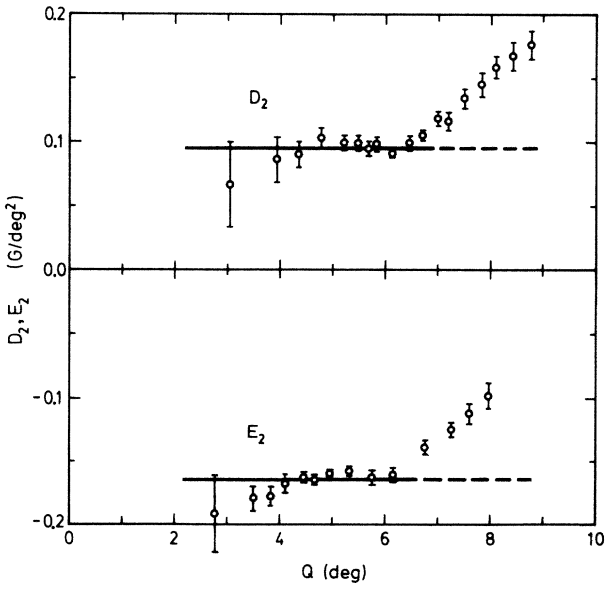

FIG. 5. Parameters D_2 and E_2, representing modification of D and E with the rotation according to Eq. (4), vs Q.

IV. DISCUSSION

We have seen that the measured EPR spectra are excellently described on the basis of an incommensurate modulation wave involving rotations of the $ZnCl_4$ tetrahedra. We have further seen that these rotations are accompanied by small modifications of D and E. In this section, we discuss a few aspects of the results in relation to the incommensurate phase transition.

We first emphasize that in the fits the incommensurate modulation was chosen according to a plane wave. It is, of course, difficult to quantify any deviation from the plane-wave limit, but it is clear from the quality of the fits that such deviations as due to pinning of the incommensurate modulation to the Mn^{2+} centers cannot be present to an appreciable amount. The quantities D_2 and E_2 permit some conclusions to be drawn about the variation of the tetrahedral bond lengths and angles. Although the elements of the D tensor of Mn^{2+} in various surroundings are known to contain contributions nonlinear in the axial field,[19] i.e., the local deviations from cubic or tetrahedral symmetry, they nevertheless are a reasonable measure for these modifications. At $Q=6°$, for instance, we thus find a modification of order 1%, amounting to additional distortions of order 0.002 Å in the bond lengths, or 0.07° in the bond angles.

It is of interest to compare the measured temperature dependence of the order parameter in the incommensurate phase with theory. Since the true critical regime is expected to be very narrow,[20] a classical Landau approach should be appropriate in the range of temperatures considered. In the simplest form of the Landau theory of second-order phase transitions, the free-energy density is expanded up to fourth order in the order parameter, leading to a power law $Q \propto (T-T_1)^{\beta}$ with $\beta=0.5$, i.e., a linear dependence of Q^2 on the temperature, at variance with experiment (Fig. 4). More elaborate Landau theories encompassing both the normal-to-incommensurate and lock-in transitions have been developed.[21,22] Eliminating the spatial dependence of the incommensurate wave, one arrives at an expression for the free-energy density valid around the normal-to-incommensurate transition, reading

$$F=\frac{a_0}{2}(T-T_1)Q^2+\frac{b}{4}Q^4+\frac{c}{6}Q^6 , \tag{5}$$

with a_0, b, and $c>0$. Below T_1, minimizing F then yields

$$Q(T)=\left\{-\frac{b}{2c}+\left[\left(\frac{b}{2c}\right)^2+\frac{a_0}{c}(T_1-T)\right]^{1/2}\right\}^{1/2} . \tag{6}$$

Close to the transition, this expression approaches a power law with $\beta=0.5$. Further away from the transition it resembles a power law with $\beta=0.25$. The best fit of Eq. (6) to the results for Q, shown in Fig. 4, yields $T_1=30.42\pm0.04$ °C, $b/2c=11.8\pm2.6$, and $(a_0/c)^{1/2}=27.7\pm1.4$ $K^{-1/2}$. Evidently, the Landau theory excellently accounts for the experiments, provided an adequate form of the free-energy density is adopted. A similar conclusion has been reached by Petersson and Schneider,[22] who considered the order parameter in Rb_2ZnCl_4 down to -80 °C, yet exclusive of the regime so close to T_1 that β approaches 0.5. As a final comment, we note that the success of the Landau theory clearly detracts from the more common approach of a description of the increase of Q below T_1 in terms of a critical exponent, although a simple power law such as the one with exponent $\beta=0.35$ derived from the $3D$ XY model leads to an adequate description[8,15] of the order parameter versus the temperature with a T_1 identical to the Landau value (Fig. 4).[23]

ACKNOWLEDGMENTS

The authors wish to thank Professor A. G. M. Janner and Dr. J. I. Dijkhuis for useful discussions, and G. J. Dirksen for crystal growing. The work has been supported by the Netherlands Foundations Fundamenteel Onderzoek der Materie (FOM) and Zuiver Wetenschappelijk Onderzoek (ZWO).

[1] Y. Yamada and N. Hamaya, J. Phys. Soc. Jpn. **52**, 3466 (1983).
[2] A. C. R. Hogervorst, Ph.D. thesis, Delft University, 1986.
[3] K. Itoh, A. Hinasada, H. Matsunaga, and E. Nakamura, J. Phys. Soc. Jpn. **52**, 664 (1983).
[4] M. Quilichini and J. Pannetier, Acta Crystallogr. **B39**, 657 (1983).
[5] K. Gesi and M. Iizumi, J. Phys. Soc. Jpn. **46**, 697 (1979).
[6] H. Mashiyama, S. Tanisaki, and K. Hamano, J. Phys. Soc. Jpn. **50**, 2139 (1981); **51**, 2538 (1982).
[7] R. Blinc, V. Rutar, B. Topic, F. Milia, I. P. Aleksandrova, A. S. Chaves, and R. Gazzinelli, Phys. Rev. Lett. **46**, 1406 (1981).
[8] R. Blinc, I. P. Aleksandrova, A. S. Chaves, F. Milia, V. Rutar, J. Seliger, B. Topic, and S. Zumer, J. Phys. C **15**, 547 (1982).
[9] E. Schneider, Solid State Commun. **44**, 885 (1982).
[10] R. Blinc, B. Lozar, F. Milia, and R. Kind, J. Phys. C **17**, 241 (1984).
[11] B. W. van Beest, A. Janner, and R. Blinc, J. Phys. C **16**, 5409 (1983).
[12] M. Pezeril, J. Emery, and J. C. Fayet, J. Phys. Lett. (Paris) **41**, L499 (1980); M. Pezeril and J. C. Fayet, *ibid.* **43**, L267 (1982); A. Kaziba, M. Pezeril, J. Emery, and J. C. Fayet, Ferroelectrics **53**, 261 (1984); J. Phys. Lett. (Paris) **46**, L387 (1985).
[13] A. Kaziba and J. C. Fayet, J. Phys. (Paris) **47**, 239 (1986).
[14] T. M. Bochkova, O. E. Bochkov, S. A. Flerova, and M. P. Trubitsyn, Fiz. Tverd. Tela (Leningrad) **26**, 2170 (1984) [Sov. Phys. Solid State **26**, 1315 (1984)].
[15] E. Schneider and J. Petersson, Z. Phys. B **46**, 169 (1982).
[16] B. Bleaney and R. S. Rubins, Proc. Phys. Soc. (London) **77**, 103 (1961); **78**, 778(E) (1961); H. W. de Wijn and R. F. van Balderen, J. Chem. Phys. **46**, 1381 (1967).
[17] N. Yamada and T. Ikeda, J. Phys. Soc. Jpn. **53**, 2555 (1984).
[18] R. Blinc, Phys. Rep. **79**, 331 (1981).
[19] H. Watanabe, Prog. Theor. Phys. **18**, 405 (1957).
[20] V. L. Ginzburg, A. A. Sobyanin, and A. P. Levanyuk, in *Light Scattering Near Phase Transitions,* edited by H. Z. Cummins and A. P. Levanyuk (North-Holland, Amsterdam, 1983), Chap. 1.
[21] Y. Ishibashi, J. Phys. Soc. Jpn. **51**, 1220 (1982).
[22] J. Petersson and E. Schneider, Ferroelectrics **53**, 297 (1984).
[23] In case the exponent is left to vary, we find $\beta=0.31\pm0.03$ from adjustment of a simple power law.